



Garrad, M., Chen, H-Y., Conn, A. T., Hauser, H., & Rossiter, J. (2021). Liquid metal logic for soft robotics. *IEEE Robotics and Automation Letters*, 6(2), 4096-4103. [9384170].
<https://doi.org/10.1109/LRA.2021.3068118>

Peer reviewed version

License (if available):
CC BY

Link to published version (if available):
[10.1109/LRA.2021.3068118](https://doi.org/10.1109/LRA.2021.3068118)

[Link to publication record in Explore Bristol Research](#)
PDF-document

This is the final published version of the article (version of record). It first appeared online via IEEE at 10.1109/LRA.2021.3068118. Please refer to any applicable terms of use of the publisher.

University of Bristol - Explore Bristol Research

General rights

This document is made available in accordance with publisher policies. Please cite only the published version using the reference above. Full terms of use are available:
<http://www.bristol.ac.uk/red/research-policy/pure/user-guides/ebr-terms/>

Liquid Metal Logic for Soft Robotics

Martin Garrad^{1,3,*}, Hsing-Yu Chen^{2,3,*}, Andrew T. Conn^{2,3}, Helmut Hauser^{1,3} and Jonathan Rossiter^{1,3}

Abstract—While there are many soft matter sensing and actuation technologies, there is far less choice when it comes to soft material devices for control and computation. One solution is the Soft Matter Computer (SMC) which can perform both analogue and digital computations in soft materials. This computer processes a fluidic input pattern consisting of alternating regions of conducting and insulating fluids into an electronic output signal. However, the use of salt water as the conductive fluid means that the Soft Matter Computer has high electrical resistance and requires an AC voltage, making untethered operation impractical. In this paper, we introduce the liquid metal Soft Matter Computer (LM-SMC), which uses galinstan as an alternative conductive fluid. We show that by switching to a liquid metal-sodium hydroxide fluidic input, we reduce the electrical resistance of the SMC by three orders of magnitude, allowing operation at DC voltages of 2 Volts and under. We characterise the stability of the liquid metal input patterns and demonstrate the potential of the LM-SMC by using it to control bipolar ionic polymer metal composite and shape memory alloy actuators. By enabling fully soft computation and control of multiple actuators from a single low voltage DC source, the LM-SMC enables a new class of intelligent and untethered soft machines.

Index Terms—Liquid metal, soft robotics, soft computer, soft controller

I. INTRODUCTION

The advantages of using soft materials in robotics has led to the introduction of a plethora of soft material mechanisms for sensing and actuation [1]–[5]. However, soft material mechanisms for control and computation, which are necessary for combining these components into integrated soft robotic systems, have received less attention. As the use of rigid electronics means sacrificing some of the benefits of using soft materials, there is now growing interest in fully soft mechanisms for control and computation [6].

These mechanisms can be categorised into two main approaches: (micro-)fluidic and embodied. In the fluidic approach, digital pneumatic circuits are used to implement simple control algorithms. For example, Wehner et al. used a microfluidic circuit to control the arms of a soft octopus [7], while Mahon et al. used a similar approach to control the gait of a tripod walker [8]. On a larger scale, fluidic systems

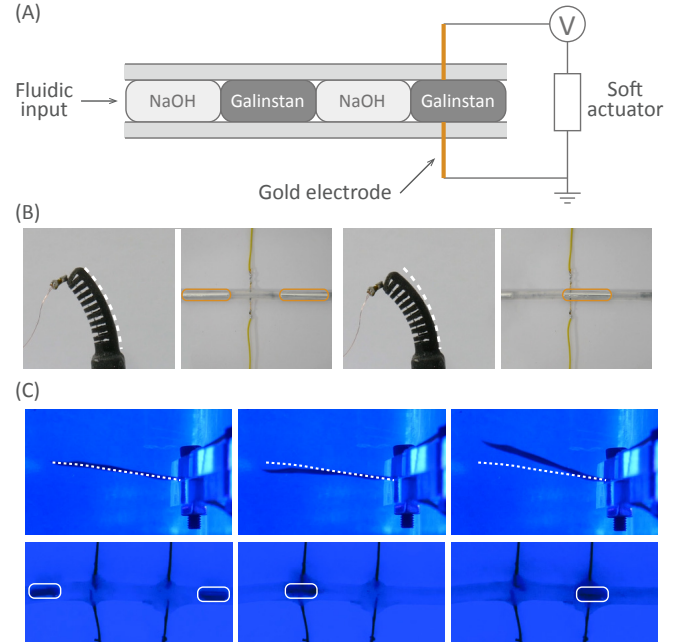


Fig. 1. Liquid metal logic. (A) Working principle of the LM-SMC. A fluidic input consisting of sodium hydroxide and liquid metal is transduced into an electrical output, controlling a soft actuator placed in series with the LM-SMC electrodes. (B) LM-SMC control of a SMA driven soft finger. When the conductive fluid (orange line) enters the electrode region, the electrical circuit is completed, causing the soft finger to bend. (C) Bi-directional control of an IPMC. When the conductive fluid (white line) enters the first electrode region, the resulting current causes the IPMC to bend upwards. When the conductive fluid enters the second electrode region, the resulting current causes the IPMC to bend downwards. In both (B) and (C), the white dashed lines represent the resting position of the actuator.

have been used to implement soft versions of fundamental electronic components, including a soft, bistable valve [9], a soft ring oscillator [10], a fluidic multiplexer [11] and both volatile and non-volatile memory [12], [13]. Finally, a self-excited soft valve has been used to generate travelling waves in a soft pneumatic robot [14].

The digital pneumatic approach inherits the large body of theory developed for digital electronics and defines a clear pathway for scaling up into more capable control systems. However, this would require overcoming current limitations in the fabrication of complex integrated pneumatic systems, and digital pneumatic circuits are currently limited to the control of pneumatic actuators.

The second main approach to controlling soft material robots - embodied control - exploits the *mechanical intelligence* of the robot's body to produce behaviours. Examples of this approach include passive dynamic walkers [15], the

*These authors contributed equally

Corresponding author: m.garrad@bristol.ac.uk

MG and HH were supported by the Leverhulme Trust Research Project RPG-2016-345. AC was supported by EPSRC research grant EP/R02961X/1. JR was supported through EPSRC research grants EP/S026096/1, EP/R02961X/1 and EP/M020460/1, and by the Royal Academy of Engineering as a Chair in Emerging Technologies.

¹Department of Engineering Mathematics, University of Bristol, UK

²Department of Mechanical Engineering, University of Bristol, UK

³SoftLab, Bristol Robotics Laboratory, University of Bristol and University of the West of England, UK

Data are available at the University of Bristol data repository, data.bris, at <https://doi.org/10.5523/bris.1x2rxzq7q9xcv22osl6vpg7bpx>.

closed loop control of a silicone octopus arm [16] and the gait transitions of a variable stiffness snake robot [17]. However, while robots which exploit their embodiment are often elegant and energy-efficient, there is no clear set of design principles which can be followed to produce an embodied control scheme that implements a target behaviour.

Recently, a third, electro-fluidic approach, known as the Soft Matter Computer (SMC, see Figure 1) [18] has been developed. An SMC consists of a number of electrode pairs patterned along a flexible tube. When an input consisting of alternating lengths of conducting and insulating fluid is injected into this tube, the electrodes transform the information in the fluidic input into an electronic control signal.

By using a fluidic input, we reduce the separation between material and computational substrates and allow the control of electrical soft actuators without requiring rigid electronic components. Fluidic inputs to the SMC may be pre-loaded into a closed tube and advanced by external mechanical pressure or driven by a soft pump [19]–[21]. This leads to the repeated execution of a fixed SMC *program*, for example, creating an oscillatory signal that could be used to control locomotion.

Previous versions of the SMC used salt water as a conductive fluid. This meant the SMC had high electrical resistance, meaning the SMC required high voltages to supply enough power to any connected actuators. Furthermore, an AC voltage source was required to prevent electrolysis of the salt water and consequent disruption of the input pattern. This requirement added complexity to the SMC drive electronics, and meant SMC controlled soft robots were either tethered, or included additional rigid electronic components. Here, we introduce the liquid metal Soft Matter Computer (LM-SMC), which replaces the salt water with liquid metal, reducing the electrical resistance by three orders of magnitude and eliminating the need for an AC voltage source. Together, these benefits make the LM-SMC a step towards a new class of intelligent and untethered soft machines.

The main contributions of this paper are:

- Introducing the concept of the LM-SMC as a step towards untethered, autonomous soft robots.
- Characterising the fluidic and electronic performance of the LM-SMC, showing increased performance over previous versions.
- Demonstrating low voltage control of a shape memory alloy driven soft finger and bipolar ionic polymer metal composite actuator.

We proceed by briefly reviewing the operating principles of the SMC and discussing the changes required by the switch to liquid metal. Next, we characterise the effect of using liquid metal as a conductive fluid upon both the electrical and fluidic properties of the SMC, showing that liquid metal is a superior alternative to salt water, significantly reducing Ohmic losses and eliminating the need for an AC voltage source. Finally, we illustrate the potential of the LM-SMC by using it to control two commonly used soft actuators: first, a shape memory alloy (SMA) driven soft finger is controlled from a 2 V DC source, and second, a pair of ionic polymer metal composite (IPMC)

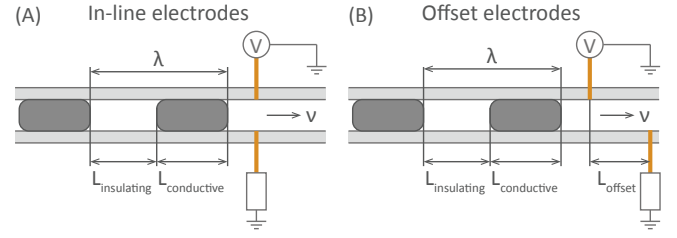


Fig. 2. **SMC Principle of operation.** A fluidic input consisting of alternating regions of conducting and insulating fluids is injected into a tube patterned with electrodes. The electrodes may be (A) in-line or (B) offset. The output of the SMC depends on both the electrode configuration and the input pattern.

actuators, which require DC voltages for bi-directional control, are switched between in- and out-of phase beating.

II. PRINCIPLE OF OPERATION

An SMC consists of one or more conductive fluid receptors (CFRs) and a fluidic input. The fluidic input consists of alternating regions of conductive and insulating fluids, where the length of each region encodes information. A conductive fluid receptor consists of pairs of electrodes embedded into a flexible tube. The electrodes may be in-line with each other (Figure 2A), or separated (Figure 2B) by a distance, L_{offset} . When the conducting fluid enters the receptor region, the electrical circuit is closed, transducing the fluidic signal into an electronic signal that can control any electrically driven soft actuators connected in series with the CFR electrodes.

Soft matter computers operate in either digital or analogue mode. When operating in digital mode, an SMC outputs zero when the insulating fluid is within the receptor region, and one when the conducting fluid is within the receptor region. Digital SMCs can be composed into units for computing logical functions with the use of an electro-fluidic diode [22].

When operating in analogue mode, the input pattern to the SMC is best viewed as a pulse-width modulated signal (PWM), consisting of a repeating pattern of wavelength λ , with a fraction of the pattern denoted by D_{in} consisting of conductive fluid. This translates to a repeating pattern of conductive fluid of length $L_{\text{conductive}} = \lambda D_{\text{in}}$ and insulating fluid of length $L_{\text{insulating}} = \lambda(1 - D_{\text{in}})$. The input flows through the SMC at a fixed rate, ν , and is mapped to a pulse-width modulated output signal of the same wavelength, but with duty fraction increased for in-line electrodes and decreased for offset electrodes.

In previous work, we used saturated salt water as the conducting fluid and air as the insulating fluid. The use of salt water meant that the SMC had a large resistance in comparison to the resistance of the actuators it was controlling. For example, we measured CFR resistances ranging from 10 - 200 Ω , depending on the magnitude of L_{offset} [18]. This meant that when driving SMA actuators, for example, voltages between 8-10 V were required to deliver sufficient current to heat the SMA above its transition temperature. Furthermore, the use of high voltages meant that using DC power sources would cause significant electrolysis, disrupting the SMC's

fluidic input pattern. To overcome this, previous versions of the SMC required an AC voltage source. The additional electronics required to generate this signal severely limited the ability to operate the SMC untethered, and completely prevented control of actuators such as IPMCs which require bipolar control signals.

In this work, we explore the use of liquid metal as an alternative conducting fluid. Specifically, we use galinstan due to its low electrical resistance, low toxicity, and the large body of recent work investigating its potential in soft robotics [23]. When gallium based liquid metals are exposed to oxygen, a rigid gallium oxide layer rapidly forms on the surface, stabilising the liquid metal [24]. This phenomenon meant air could not be used as the insulating fluid as the input did not maintain its structure as it flowed through the LM-SMC. To overcome this, we used aqueous sodium hydroxide (NaOH) for the insulating fluid, as strong acids or bases can remove this oxide layer [25].

While liquid metals do not undergo electrolysis, passing a current through sodium hydroxide causes electro-chemical reactions which produce gases at both electrodes. However, as this gas is produced in the insulating fluid of the SMC, at low rates of gas production, the transformation between fluidic input and electrical output is not disrupted. This means that it is also possible to operate the LM-SMC with DC voltages.

We also found we were able to modify the shape of the SMC electrodes when using liquid metal. When using salt water as a conducting fluid, we used *U*-shaped electrodes to create a large surface area between the salt water and electrodes and to ensure that sufficient current would flow through the SMC. When using liquid metal we found that the larger conductivity of the liquid metal made this configuration unnecessary, allowing straight electrodes (perpendicular to the direction of fluid flow) to be used. This simplified fabrication of LM-SMCs, eliminating the need to cast SMCs in two halves which are later joined together, and allowing all examples in this paper to be fabricated by hand, taking less than 30 minutes per SMC (compared to the approximately 1 hour of manual fabrication and 24 hours cure time for the original SMC).

However, we found that operation of the SMC was sensitive to electrode depth. Figure 3 shows the resulting flows for three depths of electrode. In (A), the pins cover the entire diameter of the tube, causing the conductive fluid to break into distinct sections. In (B), the electrodes are inserted to the mid-point of the tube. Here, the affinity of the liquid metal for the metal electrode caused disruption of the conducting fluid. Finally, in (C), the electrodes are inserted through the tube wall and then withdrawn such that only the tip is in contact with the fluidic input. This configuration did not disrupt the flow of the input, and is used throughout the remainder of this paper. Note that while the SMC was sensitive to the penetration depth of the electrodes, we did not find it was necessary to precisely control penetration depth, with hand fabrication and visual feedback sufficient to achieve functional LM-SMCs.

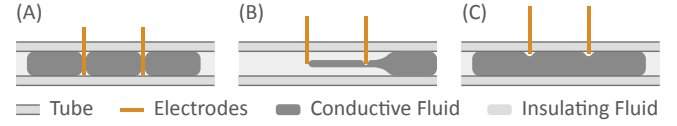


Fig. 3. **Configurations of electrodes** (A), the electrodes are inserted through the full depth of the tube. This configuration causes a breakdown of the conductive regions as they pass through the CFR region. (B), the electrodes are inserted to the mid point of the tube. This causes the liquid metal to remain attached to the electrode, again disrupting the CFR input pattern. (C), the electrodes are inserted such that they barely break the tube wall. This configuration does not disrupt the input pattern.

III. CHARACTERISATION

For stable operation of the SMC, the information in the fluidic input must be accurately and reliably mapped to an electrical output signal. Furthermore, the ratio of resistances in the insulating ($R_{\text{insulating}}$) and conducting ($R_{\text{conducting}}$) output states must be large enough to make these states distinct. In this section, we demonstrate that both of these requirements are met for a LM-SMC.

A. Fluidic characterisation

Initially, we injected fluidic inputs into tubes without CFR electrodes to remove any potential effects of electrode interaction on the flow of the input. We found that for low concentrations ($< 0.01\text{M}$) of NaOH, stable flow was not possible as the gallium oxide layer would only partially dissolve, disrupting the input pattern. At concentrations of 0.01M NaOH and above, stable flow was possible. We found that higher concentrations of sodium hydroxide increased the stability of the flow and so we used 1M NaOH as the insulating fluid throughout the rest of this paper. In contrast to the salt water SMC, we found the liquid metal input was less affected by the flow rate. Although we were able to disrupt the input when driving the flow manually, the pattern remained stable when driven at the maximum rate ($26.67 \text{ cm}^3 / \text{s}$) of our syringe drivers.

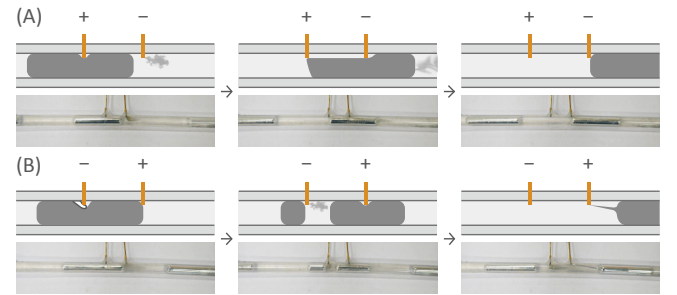


Fig. 4. **Input stability and electrode configuration.** In (A), the liquid metal encounters the positive electrode first. This leads to a small amount of electrolysis in the insulating fluid, but does not disrupt the input pattern. In (B), the liquid metal encounters the negative electrode first. This leads to a large amount of electrolysis as the liquid metal approaches the positive electrode, disrupting the input pattern. Later, the two segments re-join after entering CFR but a large tail remains connected to the positive electrode when leaving.

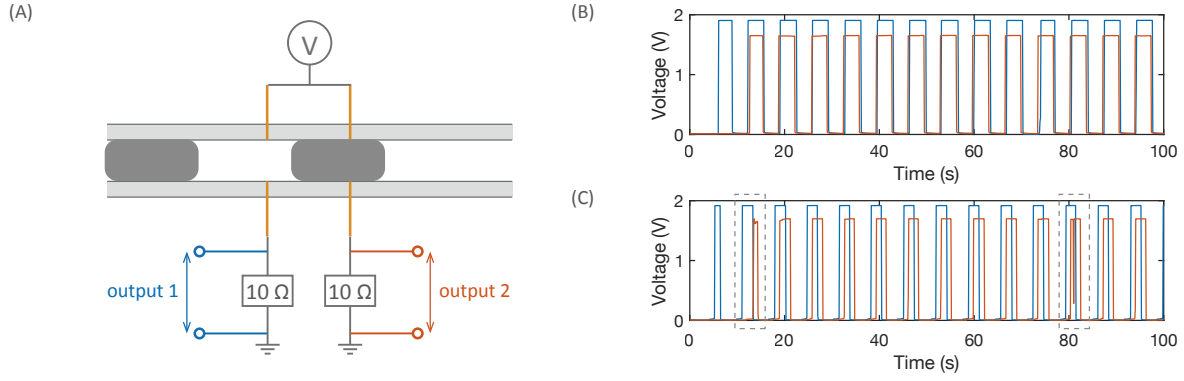


Fig. 5. **Fluidic characterisation.** (A) shows the experimental setup used to measure the stability of the fluidic input. (B) shows the output for an applied voltage of 2 V, with the blue line showing the output at electrode 1 and the red line shows the output at electrode 2. (C) plots the output for the same input but with electrodes offset by $L_{\text{offset}} = 10$ mm. Highlighted regions show cycles where the output has split into two smaller duty factor regions.

When we inserted CFR electrodes and applied a voltage across them we identified two phenomena that had the potential to disrupt stable operation. First, we found that a large amount of electrolysis occurred when operating at higher DC voltages (> 2.5 V). At lower voltages, electrolysis still occurred, but did not appear to disrupt stable operation with in-line electrodes. However, we found that offset electrodes could lead to electrolysis even at low voltages as the liquid metal region of the input approached the second electrode as shown in Figure 4. We believe this is due to the effective resistance of the sodium hydroxide solution reducing as the liquid metal approaches the second electrode, allowing a greater current to

flow, in turn leading to more gas production.

Second, we noticed that the liquid metal displayed anodophilic behaviour. This manifested itself in two ways. Firstly, when the liquid metal was leaving the positive electrode, it would experience a small force pulling it back towards the electrode. At low flow rates ($< 3.33 \text{ cm}^3 / \text{s}$), this could prevent the liquid metal from detaching from the electrode. To avoid this condition, we maintained flow rates above $10 \text{ cm}^3 / \text{s}$ for all experiments in this paper. We also found that when the liquid metal detached from the positive electrode, a thin filament would remain connected to the positive electrode, as shown in Figure 4B. As the liquid metal moved away from the electrode, this filament would increase in length, until suddenly detaching from the main liquid metal slug. Upon detaching from the main slug, the filament would form a small bead of liquid metal that remained on the positive electrode. This effect could transfer liquid metal from one slug to the next, disrupting the stability of the fluidic input. This effect was sensitive to the configuration of electrodes and the voltage across the electrode pair. We also found this effect was stronger for offset electrodes and the input was significantly less likely to be disrupted if it encountered the positive electrode before the negative electrode (Figure 4A).

To assess how these two phenomena affected the quality of the output signal and to define the operating parameter space of the LM-SMC, we conducted three experiments, measuring the change in output caused by electrode interaction, accuracy of input-output mapping, and long-term stability of the input. In all experiments, we used silicone tubing (3 mm inner diameter, 5 mm outer diameter), with electrodes made of 0.5 mm diameter gold plated copper wire and inserted by hand. Electrodes were sealed in place with a small amount of Sil-poxy (Smooth-on). The fluidic input was generated by two syringe pumps (World Precision Instruments AL-1000) controlled via a custom script and the electrical output was recorded by measuring the voltage drop across a 10Ω resistor with a data acquisition unit (USB-6001, National Instruments).

Initially, we fabricated SMCs with two electrode pairs and measured the output at both electrodes. This allowed us to

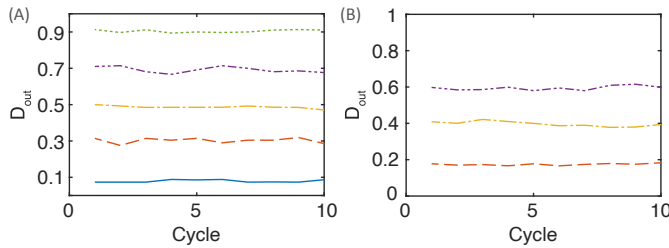


Fig. 6. **Input - Output mapping accuracy.** (A) shows the duty factor of the measured output signal for in-line electrodes, while (B) shows the duty factor for offset electrodes ($L_{\text{offset}} = 10$ mm, $v = 10 \text{ cm}^3 / \text{s}$). In both plots, we use D_{in} of 0.1 (solid blue line), 0.3 (orange dashed line), 0.5 (yellow line, dots and long dashes), 0.7 (purple line, dots and short dashes) and 0.9 (green dots). Note that when $D_{\text{in}} = 0.9$, interaction with the offset electrodes disrupted the input pattern.

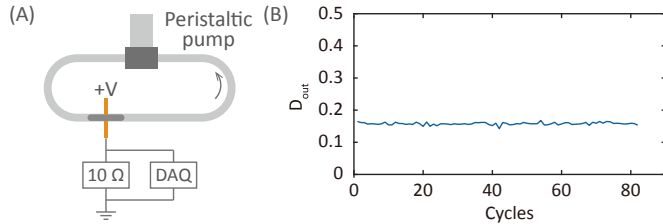


Fig. 7. **Long term stability test.** (A) shows the experimental setup, while (B) shows the measured output for each cycle.

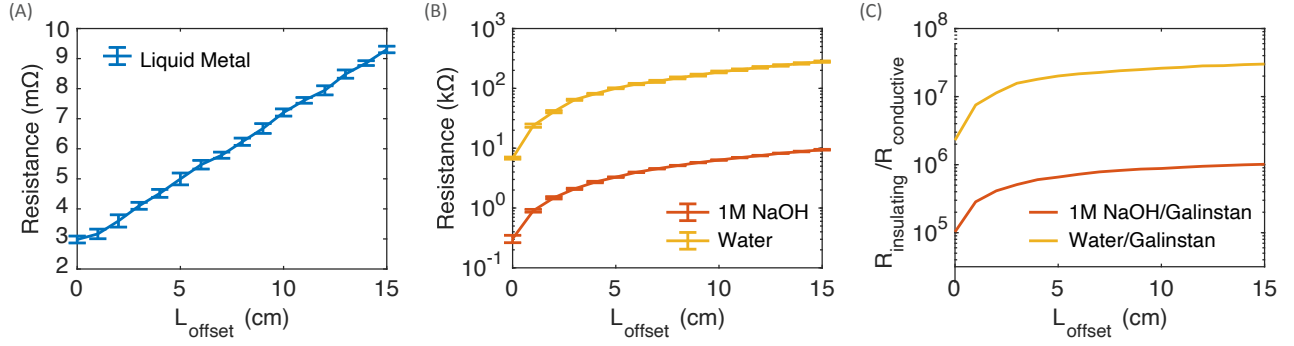


Fig. 8. **Electrical Characterisation** (A) plots the resistance of the LM-SMC when liquid metal is connecting the CFR electrodes for a range of L_{offset} . (B) plots the resistance of the LM-SMC when 1M NaOH is connecting the CFR electrodes, alongside water for comparison. (C) plots the ratio of $R_{\text{insulating}}/R_{\text{conductive}}$ as L_{offset} is increased.

quantify the change in output due to interaction with the first CFR. Figure 5A shows the experimental setup used, while 5B plots the output measured at two in-line electrodes for an input of $\lambda = 50$ mm and duty factor 0.5 at an applied voltage of 2 V. The mean difference in the duty factors measured at the two electrodes is 0.019, demonstrating interaction with the electrodes has not significantly altered the duty factor of the input signal.

At 2.5 V, we found that the fluidic input was often disrupted by interaction with the first electrode, preventing stable operation. Repeating this experiment with offset electrodes, we found that stable operation was possible at 1.5 V. However, at 2 V, a liquid metal slug would occasionally be disrupted by interaction with the electrode, leading to local errors in the output such as those shown in Figure 5C. We found that by increasing the flow rate from 10 to 26.67 cm^3/s , we were able to obtain stable flow at 2 V, and are currently investigating the relationship between flow rate and input stability further.

Next, we measured the extent to which information in the fluidic input was accurately mapped to the electrical output signal. Figure 6 plots the measured output duty factor for fluidic inputs with $\lambda = 100$ mm and duty factors of 0.1, 0.3, 0.5, 0.7 and 0.9. For in-line electrodes, we measured an output duty factor approximately equal to the input as expected. For offset electrodes ($L_{\text{offset}} = 10$ mm), the output duty factor should be reduced by $D_{\text{out}} = D_{\text{in}} - L_{\text{offset}}/\lambda = D_{\text{in}} - 0.1$. Figure 6B plots the measured output duty factor, with the output duty factor reduced by 0.1 as expected. Note that the input with $D_{\text{in}} = 0.1$ produced no output as expected. Note also that when $D_{\text{in}} = 0.9$ interaction with the offset electrodes disrupted the input pattern. Together, these results show that the fluidic input is accurately mapped to the electrical output by the LM-SMC.

Finally, we measured the long term stability of the output signal. To do this, we loaded a $D_{\text{in}} = 0.15$ input signal into a tube with in-line electrodes and an applied voltage of 1.5 V and connected it to a micro-peristaltic pump (RP-Q1 Miniature Peristaltic Pump, Takasago Electric). By comparing the change in duty factor over time, we were able to determine the stability of the fluidic input on longer time-scales. The

output signal was measured by recording the voltage drop across a 10 Ω load resistor in series with the CFR electrodes. Figure 7A shows a diagram of the experimental setup, while 7B shows the measured output duty factor, D_{out} , over 80 cycles of operation. The mean output duty factor is 0.158, with a variance of 1.5×10^{-4} , showing that long term operation of the LM-SMC is possible.

The above experiments have shown that stable LM-SMC operation is possible for a fluidic input consisting of 1M sodium hydroxide and galinstan. For in-line electrodes and DC voltages up to 2 V, fluidic inputs of at least 10 cm^3/s are accurately and reliably mapped to corresponding electrical outputs. For offset electrodes, operation is possible up to 1.5 V, provided the positive electrode is encountered before the negative electrode. By increasing the flow rate to 26.67 cm^3/s , we were able to achieve stable operation at 2 V for offset electrodes.

There are a number of soft actuators that can work at these voltages, and so can be controlled with the LM-SMC. Furthermore, as the main effect limiting SMC operation is electrolysis, we believe higher voltages would be attainable with a lower concentration sodium hydroxide solution, or alternative acid or base. We are currently investigating the effect of sodium hydroxide concentration and flow rate on the voltage limits of the LM-SMC.

B. Electrical characterisation

The operating principle of the SMC requires a conducting and insulating fluid. This means the electrical resistance of the insulating fluid must be much larger than that of the conductive fluid in order for the information encoded in the input to have the expected effect on the electrical output. Previously, we used air and salt water as the insulating and conducting fluids, and measured a ratio of resistances, $R_{\text{conducting}}/R_{\text{insulating}} > 10^6$. In this paper, we have used galinstan as a conductive fluid, with 1M sodium hydroxide as the insulating fluid. In this section, we investigate the electrical performance of the LM-SMC, showing that a liquid metal - sodium hydroxide input has the required ratio of resistances to encode information.

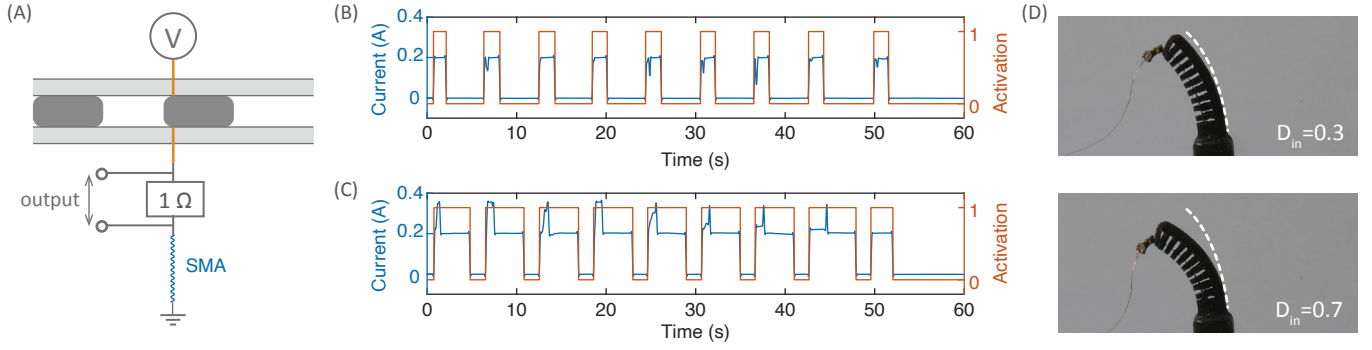


Fig. 9. **Low voltage control of an SMA driven soft finger** (A) shows the LM-SMC configuration used to control the soft finger. (B) and (C) show the current through the SMA for $D_{in} = 0.3$ and 0.7 respectively and $v = 10 \text{ cm}^3 / \text{s}$. (D) shows the soft finger for $D_{in} = 0.3$ (top) and 0.7 (bottom). The white dashed line represents the resting state of the soft finger.

To assess the electrical performance of the LM-SMC, we fabricated a number of prototypes with varying electrode offsets, L_{offset} , and measured the resistance of both liquid metal and a range of insulating fluids using an LCR meter (E4980AL, Keysight).

Figure 8A and B show the results of the measurement when the CFR region is filled with liquid metal or insulating fluid. Given the same resistivity and cross-sectional area of each specimen, the measurements increase linearly with electrode distance, agreeing with Pouillet's law. The liquid metal increases from $2.98 \text{ m}\Omega$ to $9.3 \text{ m}\Omega$ when the electrode distance increases to 15 cm . Similarly, the insulating fluids have the same tendency but in a unit of $\text{k}\Omega$. As shown in Figure 8C, the ratio of the resistances in the LM-SMC, $R_{\text{insulating}}/R_{\text{conducting}}$ is always greater than 10^5 . The difference between the two output states is therefore large enough for the electrical output to function as a control signal for a soft actuator. Furthermore, the resistance of the liquid metal is three orders of magnitude less than that measured for salt water (typically 10Ω for in-line electrodes). Consequently, for thermally driven soft actuators such as SMAs, this reduction in resistance of the LM-SMC significantly reduces the voltage required to cause actuation.

IV. SOFT ACTUATOR CONTROL DEMONSTRATIONS

We have shown that liquid metal is a superior conductive fluid for the soft matter computer, provided a sufficiently low DC voltage is used. This is because the resistance of the liquid metal is negligible, regardless of the separation between electrodes, and while the insulating fluid does allow some conduction, the ratio of resistances, $R_{\text{conducting}}/R_{\text{insulating}}$ is sufficiently large for SMC operation. Next, we show that the LM-SMC is capable of controlling two commonly used soft actuators: shape memory alloys and ionic polymer-metal composites.

A. Control of shape memory alloy powered soft fingers

First, we demonstrate control of a shape memory alloy actuator driven soft finger from a 2 V DC power source. Shape memory alloy actuators contract when heated above their transition temperature. Here, we use Joule heating to

heat an SMA attached in series with the CFR electrodes (see Figure 9A). Figure 9B and 9C show the current through the SMA for flow rates of $10 \text{ cm}^3 / \text{s}$ and $D_{in} = 0.3$ and 0.7 , respectively. We show that the magnitude of the actuation can be controlled by the LM-SMC, with a low input duty factor ($D_{in} = 0.3$) causing each finger to bend only a small amount, while a high input duty factor ($D_{in} = 0.7$) causes a much larger degree of bending, as shown in Figure 9D.

In our previous work [18], we also demonstrated control of a similar SMA driven soft finger with a fluidic input consisting of salt water and air. In that case, we required an operating voltage of 8 V to provide sufficient current to heat the SMA. Using liquid metal as the conductive fluid, we are able to actuate the same SMA at a voltage of 2 V . This is due to the significantly lower resistance of the LM-SMC. For a current of 200 mA , this is a decrease in input power required by a factor of 4. Modelling the LM-SMC as a potential divider, with the LM-SMC resistance as R_1 and the actuator as R_2 , electrical efficiency is given by the ratio $R_2/(R_1 + R_2)$. We measured 10Ω SMA resistance and $3 \text{ m}\Omega$ CFR resistance, giving an electrical efficiency of 99.97% .

B. Bi-directional control of IPMC actuators

Next, we show bi-directional control of an IPMC actuator. IPMCs are low-voltage bending actuators, ideal for use in aquatic environments. When a voltage is applied across the IPMC, migration of free positive ions causes a bending actuation [26]. Reversing the polarity of the voltage reverses the direction of bending. This requirement for a reversible polarity output meant that the high frequency AC signal of the salt water SMC was unable to control IPMCs. As the LM-SMC does not require an AC signal, this limitation can now be overcome.

Figure 10A shows the LM-SMC configuration used to control the bi-directional bending of an IPMC (Nafion 118). The LM-SMC consists of two CFRs, with one connected to the $+1.5 \text{ V}$ DC source and the second connected to a -1.5 V source. Figure 10B shows the resulting movement when an input signal with flow rate of $10 \text{ cm}^3 / \text{s}$, $\lambda = 100 \text{ mm}$ and $D_{in} = 0.5$ is applied to the LM-SMC.

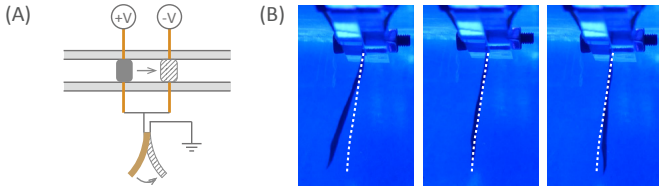


Fig. 10. **Bi-directional control of an IPMC** (A) shows the LM-SMC configuration used to control the IPMC, while (B) shows the movement of the IPMC as the conductive region moves from the first electrode (left) through the region between the CFR electrodes (middle) and finally into the second electrode (right).

We further show that the LM-SMC is capable of controlling the phase of the output of two IPMC actuators from a single DC source with constant voltage. To achieve this, we created an LM-SMC with four pairs of CFR electrodes, with two pairs of electrodes attached to each IPMC. Figure 11A shows a diagram of the LM-SMC configuration used for in-phase beating, alongside images of the resulting movement and the measured current through each IPMC. By swapping the polarity of the final two CFRs we are able to switch between in phase and out of phase beating. Figure 11B shows this setup alongside images of the movement and the control signals. Note that although we switched the polarity of the CFR electrodes manually, this could have equally been achieved by using digital mode LM-SMCs.

V. DISCUSSION & CONCLUSIONS

In this work, we have investigated the use of liquid metal as a novel conducting fluid for the input of a soft matter computer. We have shown that for DC voltages of 2 V, stable and accurate operation of the SMC is possible for in-line electrodes. For off-set electrodes, we have shown that operating voltages up to 2 V are possible provided the input has a sufficient flow rate, and the order of the electrodes must be such that the positive electrode is encountered first. While we are currently investigating the use of alternative insulating fluids to increase the maximum operating voltage, these voltages are high enough for control of some soft actuators.

We have also shown that the ratio of resistances between the insulating and conducting fluids is greater than 10^5 , meaning the electrical difference between the two output states is also sufficient for SMC operation. Moreover, the vastly reduced resistance of the LM-SMC leads to a greatly improved electrical efficiency, and eliminates the need for AC voltages. Finally, we have demonstrated the practical application of the LM-SMC by using it to control an SMA driven soft finger, and a bi-polar IPMC actuator.

In comparison to the previous version of the SMC, the LM-SMC is capable of a smaller range of computations. While the salt water SMC can have electrodes of positive or negative overlap, the LM-SMC is limited to in-line electrodes ($L_{\text{electrode}} \approx 0$) or offset electrodes. This means the duty factor of the output will always be equal or less to that of the input.

The energy efficiency of an SMC controlled actuator will depend on a number of factors: electrical losses will depend

on the operating current and voltage of the actuator, while mechanical losses will depend on the choice of fluids, tube geometry, the flow rate and the mechanism used to advance the input. Using liquid metal instead of salt-water improves the electrical efficiency of the LM-SMC; for the SMAs used in this work, we achieve a reduction in operating voltage from 8V to 2V, and a corresponding reduction in electrical power of 1.2W. However, this comes at the cost of decreased mechanical efficiency. This is due to the increased viscosity of both the conducting (galinstan 2.4 mPa-s and salt water 1 mPa-s at 20°C) and insulating (NaOH 1.227 mPa-s and air 0.0181 mPa-s at 20°C) fluids. As pressure losses due to viscous effects are proportional to the square of flow rate and the inverse of tube diameter to the fourth power, at high flow rates, or small tube diameters, these mechanical losses may offset the increased electrical efficiency of the LM-SMC.

The LM-SMC is less sensitive to the input flow rate than the original SMC, with stable flow possible at rates up to $26 \text{ cm}^3 / \text{s}$. However, unlike the original SMC, the LM-SMC requires a minimum flow rate of $10 \text{ cm}^3 / \text{s}$. This means the LM-SMC may not be suitable for applications where a slowly varying control signal is required. We believe the greater stability of the LM-SMC is due to the greater cohesive forces within the liquid metal. On the other hand, there is a greater difference in densities between the two fluids in the LM-SMC, meaning it is possible the LM-SMC is less stable when oriented vertically.

Although we have focused on analogue mode SMC computations, the reduced resistance of the LM-SMC also benefits the digital mode SMC operation by allowing the composition of a far greater number of LM-SMCs. We have previously demonstrated the ability to compose multiple digital SMCs into logic gates [18]. However, composing these gates into more complex devices was impractical as the total resistance of the combined unit was too large to drive most soft actuators without causing electrolysis of the salt water. The greatly reduced resistance of the LM-SMC means that this limitation can be overcome, allowing the possibility of combining LM-SMCs to produce a wider range of control signals.

Furthermore, unlike the previous SMC, which required AC voltages of 8-10 V to switch an SMA actuator, the LM-SMC can operate at low ($\leq 2 \text{ V}$) DC voltages. Removing the requirement for an AC signal eliminates the need for additional (rigid) electronics. Crucially, it is possible to use an LM-SMC to control both IPMC and SMA actuators at voltages below the 3.3 V provided by a coin cell battery.

To achieve untethered operation, an input pattern can be pre-loaded into an LM-SMC and driven cyclically by a soft peristaltic pump [20] or oscillating pressure source [10], [12]. This corresponds to the repeated execution of a fixed program. More complex behaviours are likely to require dynamic generation or modification of the LM-SMC input pattern, and we are currently working on such an architecture.

In this paper, we have introduced the LM-SMC, a soft computer for the control of soft robots. We have shown that information can be encoded in a liquid metal - sodium hydrox-

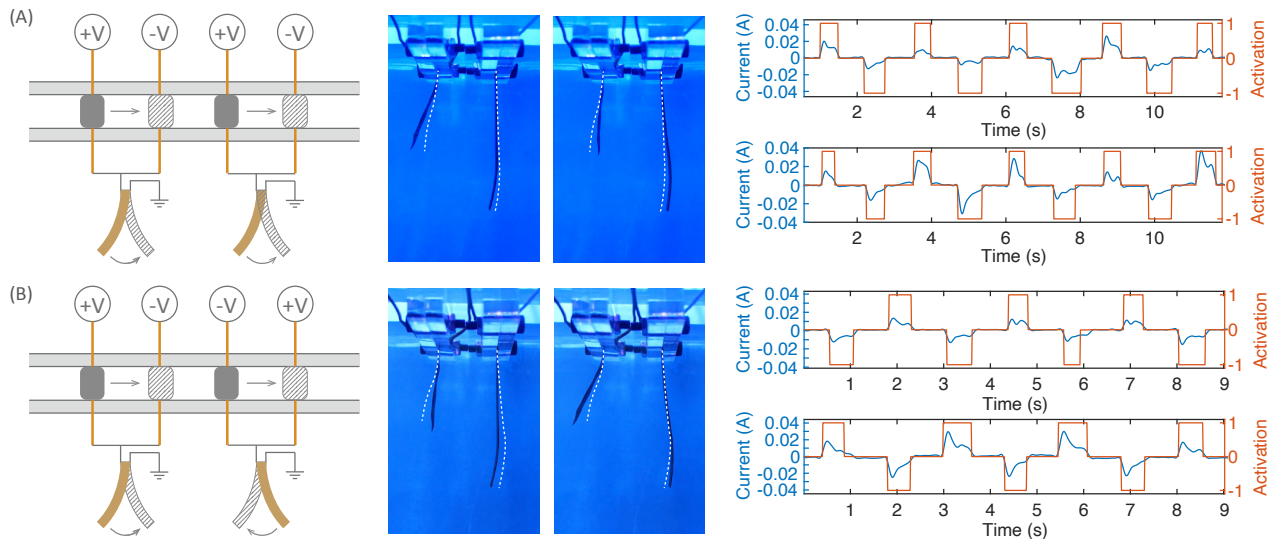


Fig. 11. **Phase-switching of two IPMCs.** (A) shows the LM-SMC configuration used for in-phase beating (left), alongside two images of the IPMC movement (middle) and the measured control signals (right) with $v = 10 \text{ cm}^3 / \text{s}$. (B) shows the same information for the out-of-phase configuration.

ide fluidic input and used this information to control a range of soft actuators. Further, we have shown that the reduced electrical resistance of the LM-SMC allows low voltage DC electrical sources to be used. This marks the LM-SMC as a step towards untethered soft robots that integrate soft sensing and actuation to produce complex autonomous behaviours.

REFERENCES

- [1] J. M. McCracken, B. R. Donovan, and T. J. White, "Materials as machines," *Advanced Materials*, vol. 32, no. 20, p. 1906564, 2020.
- [2] M. Taghavi, T. Helps, and J. Rossiter, "Electro-ribbon actuators and electro-origami robots," *Science Robotics*, vol. 3, no. 25, 2018.
- [3] H.-Y. Chen and A. T. Conn, "A stretchable inductor with integrated strain sensing and wireless signal transfer," *IEEE Sensors Journal*, vol. 20, no. 13, pp. 7384–7391, 2020.
- [4] T. G. Thuruthel, B. Shih, C. Laschi, and M. T. Tolley, "Soft robot perception using embedded soft sensors and recurrent neural networks," *Science Robotics*, vol. 4, no. 26, 2019.
- [5] C. S. Haines, M. D. Lima, N. Li, G. M. Spinks, J. Foroughi, J. D. Madden, S. H. Kim, S. Fang, M. J. De Andrade, F. Göktepe *et al.*, "Artificial muscles from fishing line and sewing thread," *Science*, vol. 343, no. 6173, pp. 868–872, 2014.
- [6] S. I. Rich, R. J. Wood, and C. Majidi, "Untethered soft robotics," *Nature Electronics*, vol. 1, no. 2, pp. 102–112, 2018.
- [7] M. Wehner, R. L. Truby, D. J. Fitzgerald, B. Mosadegh, G. M. Whitesides, J. A. Lewis, and R. J. Wood, "An integrated design and fabrication strategy for entirely soft, autonomous robots," *Nature*, vol. 536, no. 7617, pp. 451–455, 2016.
- [8] S. T. Mahon, A. Buchoux, M. E. Sayed, L. Teng, and A. A. Stokes, "Soft robots for extreme environments: removing electronic control," in *2019 2nd IEEE International Conference on Soft Robotics (RoboSoft)*. IEEE, 2019, pp. 782–787.
- [9] P. Rothmund, A. Ainla, L. Belding, D. J. Preston, S. Kurihara, Z. Suo, and G. M. Whitesides, "A soft, bistable valve for autonomous control of soft actuators," *Science Robotics*, vol. 3, no. 16, 2018.
- [10] D. J. Preston, H. J. Jiang, V. Sanchez, P. Rothmund, J. Rawson, M. P. Nemitz, W.-K. Lee, Z. Suo, C. J. Walsh, and G. M. Whitesides, "A soft ring oscillator," *Science Robotics*, vol. 4, no. 31, p. eaaw5496, 2019.
- [11] N. W. Bartlett, K. P. Becker, and R. J. Wood, "A fluidic demultiplexer for controlling large arrays of soft actuators," *Soft Matter*, 2020.
- [12] D. J. Preston, P. Rothmund, H. J. Jiang, M. P. Nemitz, J. Rawson, Z. Suo, and G. M. Whitesides, "Digital logic for soft devices," *Proceedings of the National Academy of Sciences*, vol. 116, no. 16, pp. 7750–7759, 2019.
- [13] M. P. Nemitz, C. K. Abrahamsson, L. Wille, A. A. Stokes, D. J. Preston, and G. M. Whitesides, "Soft non-volatile memory for non-electronic information storage in soft robots," in *2020 3rd IEEE International Conference on Soft Robotics (RoboSoft)*. IEEE, 2020, pp. 7–12.
- [14] Y. Miyaki and H. Tsukagoshi, "Self-excited vibration valve that induces traveling waves in pneumatic soft mobile robots," *IEEE Robotics and Automation Letters*, vol. 5, no. 3, pp. 4133–4139, 2020.
- [15] S. Collins, A. Ruina, R. Tedrake, and M. Wisse, "Efficient bipedal robots based on passive-dynamic walkers," *Science*, vol. 307, no. 5712, pp. 1082–1085, 2005.
- [16] K. Nakajima, H. Hauser, T. Li, and R. Pfeifer, "Information processing via physical soft body," *Scientific Reports*, vol. 5, p. 10487, 2015.
- [17] M. Garrad, J. Rossiter, and H. Hauser, "Shaping behavior with adaptive morphology," *IEEE Robotics and Automation Letters*, vol. 3, no. 3, pp. 2056–2062, 2018.
- [18] M. Garrad, G. Soter, A. Conn, H. Hauser, and J. Rossiter, "A soft matter computer for soft robots," *Science Robotics*, vol. 4, no. 33, p. eaaw6060, 2019.
- [19] C. D. Onal, X. Chen, G. M. Whitesides, and D. Rus, "Soft mobile robots with on-board chemical pressure generation," in *Robotics Research*. Springer, 2017, pp. 525–540.
- [20] G. Mao, X. Huang, J. Liu, T. Li, S. Qu, and W. Yang, "Dielectric elastomer peristaltic pump module with finite deformation," *Smart Materials and Structures*, vol. 24, no. 7, p. 075026, 2015.
- [21] V. Caciucio, J. Shintake, Y. Kuwajima, S. Maeda, D. Floreano, and H. Shea, "Stretchable pumps for soft machines," *Nature*, vol. 572, no. 7770, pp. 516–519, 2019.
- [22] M. Garrad, G. Soter, A. T. Conn, H. Hauser, and J. Rossiter, "Driving soft robots with low-boiling point fluids," in *2019 2nd IEEE International Conference on Soft Robotics (RoboSoft)*. IEEE, 2019, pp. 74–79.
- [23] J. Yan, Y. Lu, G. Chen, M. Yang, and Z. Gu, "Advances in liquid metals for biomedical applications," *Chemical Society Reviews*, vol. 47, no. 8, pp. 2518–2533, 2018.
- [24] M. D. Dickey, "Emerging applications of liquid metals featuring surface oxides," *ACS Applied Materials & Interfaces*, vol. 6, no. 21, pp. 18 369–18 379, 2014.
- [25] M. R. Khan, C. B. Eaker, E. F. Bowden, and M. D. Dickey, "Giant and switchable surface activity of liquid metal via surface oxidation," *Proceedings of the National Academy of Sciences*, vol. 111, no. 39, pp. 14 047–14 051, 2014.
- [26] M. Shahinpoor, Y. Bar-Cohen, J. Simpson, and J. Smith, "Ionic polymer-metal composites (ipmcs) as biomimetic sensors, actuators and artificial muscles-a review," *Smart Materials and Structures*, vol. 7, no. 6, p. R15, 1998.